IEEE Photonics Journal
An IEEE Photonics Society Publication

Automatic Identification of Malaria-Infected RBC With Digital Holographic Microscopy Using Correlation Algorithms

Volume 4, Number 5, October 2012

A. Anand
V. K. Chhaniwal
N. R. Patel
B. Javidi, Fellow, IEEE

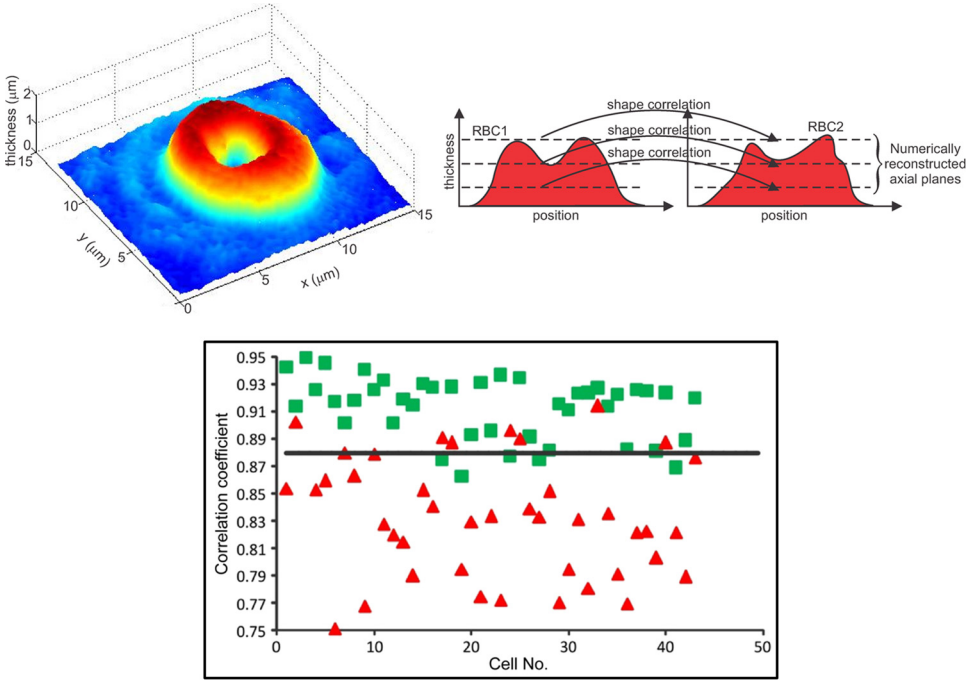

DOI: 10.1109/JPHOT.2012.2210199
1943-0655/$31.00 ©2012 IEEE

Automatic Identification of Malaria-Infected RBC With Digital Holographic Microscopy Using Correlation Algorithms

A. Anand,[1] V. K. Chhaniwal,[1] N. R. Patel,[1] and B. Javidi,[2] *Fellow, IEEE*

[1]Optics Laboratory, Department of Applied Physics, Faculty of Technology and Engineering, MS University of Baroda, Vadodara 390001, India
[2]Department of Electrical and Computer Engineering, U-2157, University of Connecticut, Storrs, CT 06269-2157 USA

DOI: 10.1109/JPHOT.2012.2210199
1943-0655/$31.00 ©2012 IEEE

Manuscript received June 30, 2012; accepted July 20, 2012. Date of publication July 31, 2012; date of current version August 7, 2012. The work of A. Anand was supported by departmental research grants from University Grants commission, Government of India and Department of Science and Technology, Government of India. Corresponding author: A. Anand (e-mail: arun_nair_in@yahoo.com).

Abstract: Diagnosis of malaria is important for its medication and treatment. An automatic compact diagnostic tool will be advantageous especially for healthcare personnel working in developing countries, which lack trained professionals and high-quality equipments. Digital holographic microscopy is one of the advanced techniques for quantitative evaluation of cells, providing cell thickness information directly. This information obtained by interferometric comparison can be used to identify as well as to compare cells. Here, we describe the use of digital holographic interferometric microscopy (DHIM) with numerical focusing for automatic identification of malaria-infected red blood cells (RBCs). Identification is done by comparing its shape profile with that of a healthy RBC. A correlation function was used to separate healthy and malaria-infected RBCs.

Index Terms: Quantitative microscopy, digital holographic microscopy, coherent imaging, disease identification, correlation.

1. Introduction

Malaria is one of the most widespread and potentially fatal diseases especially in Africa and Asia. A correct diagnostics of malaria is essential for proper medication and cure. Main clinical diagnostics of malaria is based on microscopic inspection of blood smears, treated with reagents, which stains the malarial parasites. A technician visually inspects these smears to identify malaria-infected red blood cells (RBCs). In developing countries, visual identification of malarial RBCs may become unreliable due to lack of sufficiently trained technicians and poor-quality microscopes and reagents. Also, in remote areas, malaria diagnostics could benefit from the use of portable and easy-to-use instruments to automatically discriminate between malarial and healthy RBCs.

Interference techniques (two-beam, single-beam, common path) can be used for quantitative phase-contrast imaging [1]–[17]. The phase will provide thickness information of the cell. Digital holographic microscopy (DHM) is an effective tool for 3-D imaging of micro-objects [1]–[9]. This technique is based on electronic recording of holograms and their numerical reconstruction by simulating diffraction. Added advantage of this technique is numerical focusing, allowing one to focus on to any desired object plane [9]. Interferometric comparison of phases at the image plane obtained from the recorded holograms with the object present and with just the background provides

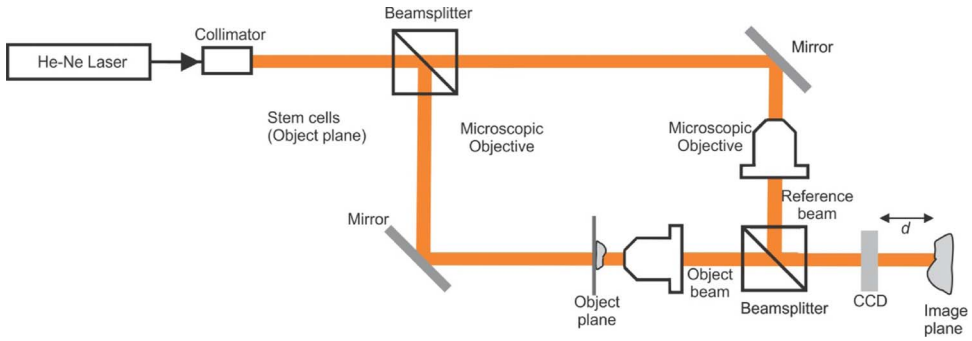

Fig. 1. Digital holographic interferometric microscope used for the investigation of RBCs.

object phase information. This can be converted into thickness information of the cells [2], [3], [7], [8], and then, numerical focusing provides thickness profile at desired planes, supplying additional information about the cell [9]. Recently, malaria-infected RBCs have been investigated in detail with quantitative phase microscopic techniques [12], [13]. Diffraction phase microscopy has also been used for blood screening [14], [15]. In these investigations, different cell parameters like its volume and hemoglobin content were extracted and used for screening of the cells.

Here, we describe the use of quantitative DHM for automatic identification of malaria-infected RBCs by comparing their shape profiles at different axial planes. A correlation algorithm discriminates between the shapes of the cells and determines whether the cell is infected by malaria parasite. Shape comparison is fast and was found to yield fairly accurate discrimination.

2. Digital Holographic Interferometric Microscope

Fig. 1 shows the digital holographic microscope used in investigating RBCs. A random linearly polarized He–Ne laser source providing CW output at 611 nm and maximum output power of 2 mW was utilized in the experiments. The laser beam was expanded and collimated. This was then split into two using a nonpolarizing beam splitter. One of the beams acts as the reference beam, and the other beam is condensed and passed through the object under investigation. A microscopic objective (Oil immersion, $100\times$, NA $= 1.25$) magnifies the object. A CCD (AVT Guppy-146C having 8-bit dynamic range, and 4.65 $\mu \times 4.65$ μ pixel size) camera was used for recording intensity patterns. The object beam and the reference beam were made to interfere at the CCD camera using a Mach–Zehnder configuration. A similar kind of focusing lens and microscopic objective is introduced in the object beam path to match the curvatures of the beams, and a slight angle is introduced between the object and reference beams to achieve off-axis geometry.

Once the holograms were recorded, it remains to reconstruct the object wave. This was achieved by simulating the diffraction of the reference beam occurring at the microstructures of the recorded hologram using scalar diffraction integral [18]. Since the digitally recorded holograms are discrete in nature (finite pixel and array size), a discrete form of the diffraction integral was used [1]. Here, since short-distance propagations are involved, an angular spectrum approach to the diffraction theory was used for reconstructions [6], [7], [18]. For microscopy of phase objects, the angular spectrum propagation (ASP) approach also makes a compact experimental setup possible. An added advantage of this method is that it can separate out the different diffracted components in the frequency domain, and hence, there will not be overlap between these components at the reconstruction plane [6].

3. Thickness Determination of RBC

Holograms of the RBC as well as the surrounding medium were recorded and reconstructed. Phase obtained from the reference hologram is numerically subtracted from the phase obtained

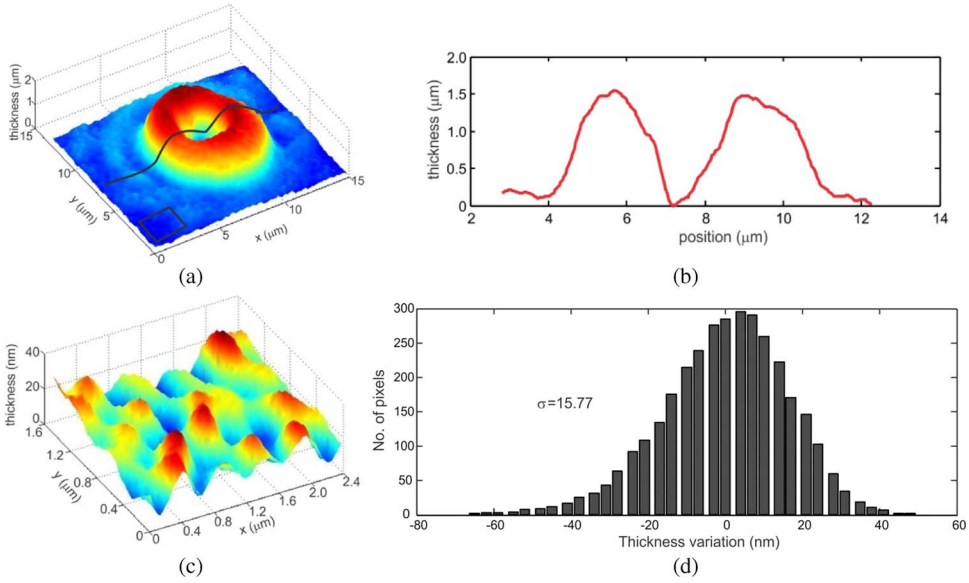

Fig. 2. (a) Computed thickness profile of a healthy RBC imaged using DHIM. (b) Cross-sectional thickness profile. (c) Thickness variation in the region marked by the rectangle in (a). (d) Histogram of the path length variation in the region where no cell was present.

from the object hologram. By doing so, one can eliminate irregularities due optics. This phase difference is related to the cell thickness through

$$\Delta\phi(x, y) = \frac{2\pi}{\lambda}(n_o - n_r)L(x, y) \tag{1}$$

where n_o and n_r are the constant refractive index of RBC and blood plasma (surrounding medium), respectively, and L is the thickness at a given point. Effective refractive indices of 1.42 and 1.34 for RBC and for the surrounding medium (plasma), respectively, were used to convert phase information into thickness information [19]. It should be noted that the thickness of the RBC was computed after unwrapping the phase distribution using the Goldstein branch-cut method, and this step can be avoided by using a multiwavelength approach [20], [21].

Blood samples were collected from healthy individuals and from individuals detected with severe malaria. These samples were centrifuged to separate malaria-infected RBCs. Thin blood smears were formed on a glass slide, and they were covered with a cover slip. And their holograms were then recorded. Fig. 2 shows the obtained thickness profile for a healthy RBC and its cross-sectional profile using DHIM. Doughnut shape of RBC is quite visible in the thickness profile. The analysis of the RBCs (healthy and malaria) was done by comparing single plane or multiple planes of healthy and diseased RBCs. Selection of different planes was done with the help of numerical focusing.

4. Cell Identification

Before identification, location of the cells in the field of view has to be determined. This is obtained from the thickness profile (average thickness of a healthy RBC in our case was between 1.5 μm and 2.2 μm). In the region where no cell is present (background), variation in thickness should be ideally zero. But due to variations occurring in the experimental setup between exposures, reconstructed phase will change, and it will reflect as a variation in thickness. The standard deviation of computed thickness in the region where no cell is present is the axial resolution of the system, and, in the present case, it was found to be less than 16 nm [see Fig. 2(d)]. So by thresholding the thickness distribution by the resolution of the system, location of the cells can be automatically determined.

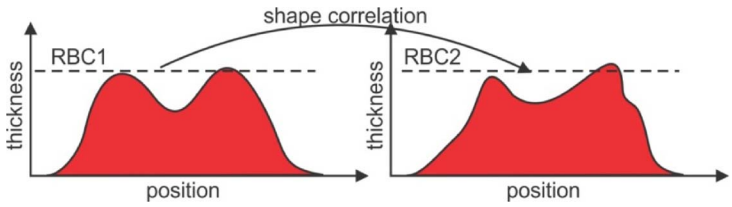

Fig. 3. Cell identification using single plane.

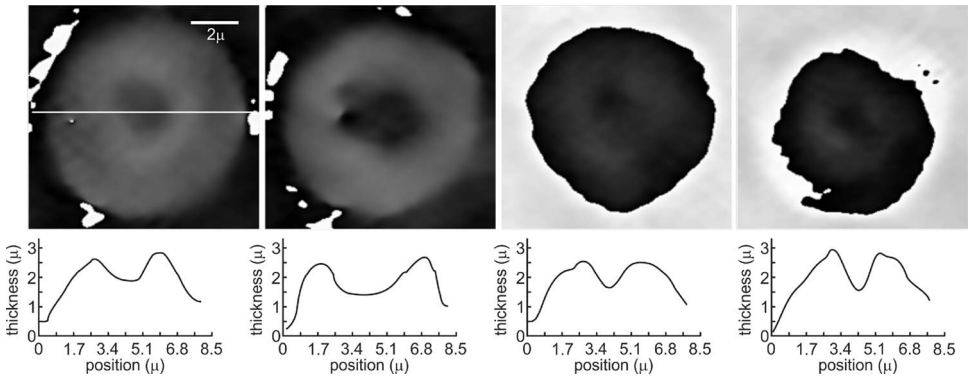

Fig. 4. Top row shows phase-contrast images of four different healthy RBCs. Bottom row depicts the cross-sectional thickness profile along the center line.

Type of the RBC (healthy or malaria infected) was determined by finding the correlation between the cell shapes. The most familiar measure of dependence between two quantities, in the present case thickness distributions, is the Pearson product-moment correlation coefficient or "Pearson's correlation." The sample correlation coefficient between two random variables X and Y is determined using

$$r_{XY} = \sum_{i=1}^{n} (x_i - \overline{x})(y_i - \overline{y})/(n-1)S_X S_Y \tag{2}$$

where $\overline{x}$ and $\overline{y}$ are the sample means of X and Y, and S_x and S_y are the sample standard deviations of X and Y. In the present case, X and Y represent the thickness variation at a particular image plane for two cells. Other types of correlation measures based on filters can also be used [22].

4.1. Identification Using Single Reconstruction Plane

Initially, identification was done using thickness information from a single axial plane (image plane) (see Fig. 3). In the present study, 43 healthy and 43 malaria-infected RBCs were used to form a database. Thickness distributions of the RBCs at the best focus plane were compared.

Fig. 4 shows the reconstructed phase maps and the cross-sectional profiles at the image plane for four different healthy RBCs. For all the RBCs, the image plane corresponded to the recording plane. Phase-contrast images for the malaria-infected RBC along with the cross-sectional profiles are shown in Fig. 5.

From Figs. 4 and 5, it is evident that the shape of the healthy RBC is different from that of the malaria-infected RBC. Healthy cells were found to have a doughnut-shaped profile, and most of the cells with malaria parasite had a convex-shaped profile. So comparing the shape of an unknown cell with the shape of healthy cells and setting a threshold for the correlation coefficient, it is possible to differentiate between healthy and malaria-infected cells. First, shape comparison of healthy RBCs with each other was done, and the average correlation coefficient was calculated for

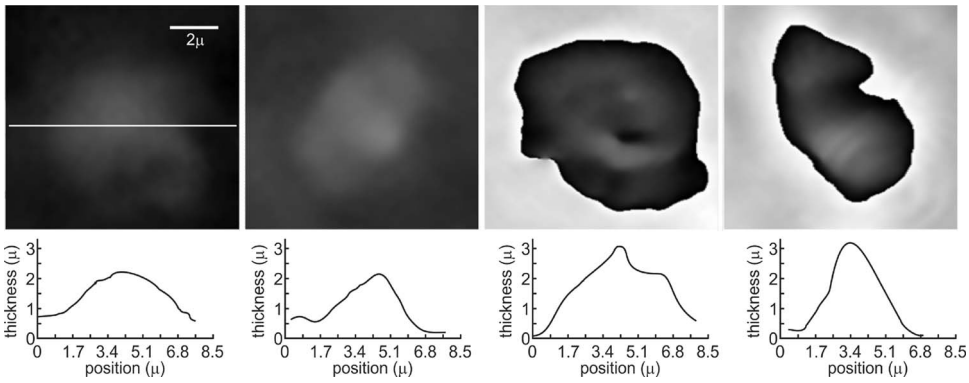

Fig. 5. Top row shows phase-contrast images of four different malaria-infected RBCs. Bottom row depicts the cross-sectional thickness profile.

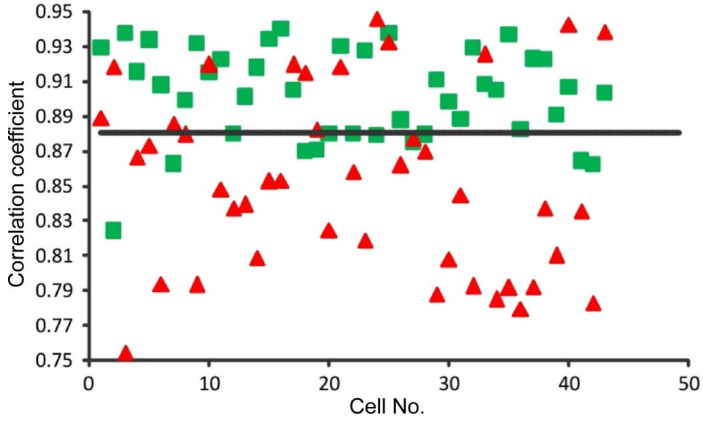

Fig. 6. Average correlation coefficient from shape comparison of different cell pairs using data from a single reconstruction plane (■ healthy, ▲ malaria infected, — threshold).

each cell. Same procedure was repeated for the malaria-infected RBCs. Then, healthy RBCs were compared with malaria-infected RBCs, and again, the average correlation coefficient was calculated. Fig. 6 shows the variation in the average correlation coefficient for different cell combinations. A threshold of 0.88 yielded the best discrimination probability and least false positive rate. With this threshold, 69% malaria-infected RBCs could be correctly identified by comparing it to the shape of healthy cells (green rectangles). False positive and false negative rates for this case were 2.7 out 10 and 3 out of 10, respectively. Table 1 shows the mean of the obtained correlation coefficients using data from single and multiple reconstructed planes as well as their standard deviations.

4.2. Identification Using Multiple Reconstruction Planes

If the two cells have same shape, it should lead to a normalized correlation value of 1. But no two cells have identical shape even though they are from the same class, and this will give rise to a correlation value less than 1. So if information from a single reconstructed plane is used for identification purpose, it may lead to an error. A better way is to find the correlation between multiple axial planes of the cell (see Fig. 7). The thickness information at different cell axial planes is obtained using the numerical focusing. A database for healthy and malaria-infected RBCs was constructed using information from multiple axial planes. Correlation between the corresponding axial planes of the cells is then computed. The average of shape correlations at all the axial planes

TABLE 1

Obtained correlation coefficient and their standard deviation (SD) for different cell combinations as well as the classification probability

RBC combination	Using single plane reconstruction plane				Using multiple reconstruction planes (20 planes)			
	Correlation coefficient		Detection probability		Correlation coefficient		Detection probability	
	Mean	SD	TPR	FPR	Mean	SD	TPR	FPR
Healthy-Healthy	0.902	0.0266	69%	27%	0.925	0.0226	84%	11%
Healthy-Malarial	0.853	0.0531			0.827	0.0525		

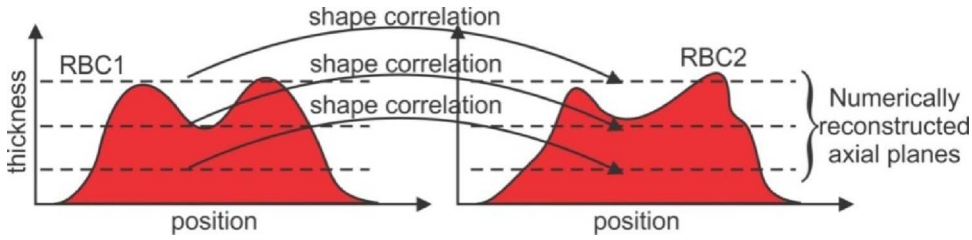

Fig. 7. Cell identification using multiple axial planes.

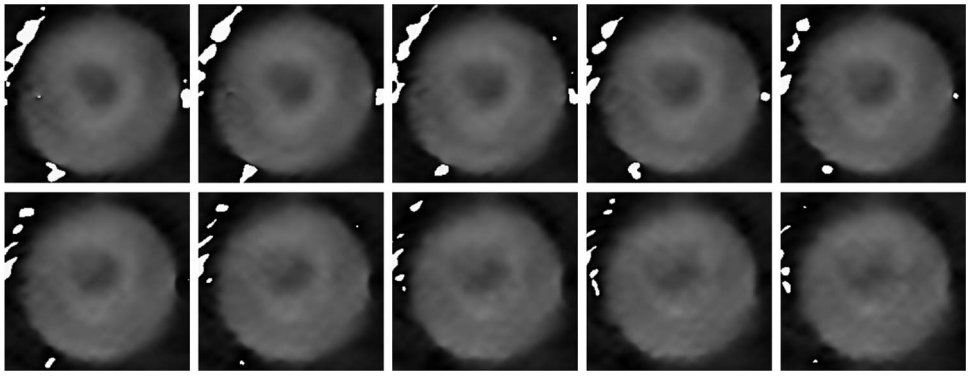

Fig. 8. Phase-contrast images of a healthy RBC obtained at various axial distances. The distance between successive axial planes was 0.24 μm.

is then taken as the correlation coefficient between the cells to be examined and the cells from the database. In the present case, thickness at 20 axial planes separated by 0.12 μm were computed to construct the database. Figs. 8 and 9 show the phase-contrast images at 10 axial planes for a healthy RBC and for malaria-infected RBCs, respectively.

Fig. 10 shows the average correlation coefficient for different cell combinations obtained using information from multiple axial planes. Here also, a threshold of 0.88, which yielded the highest probability of correct classification, was used. It can be seen that (compared with Fig. 6) the probability of correct classification has now increased to 84% and false positive and false negative rates reduced to 1.1 out of 10 and 1.6 out of 10, respectively. Also, correlation coefficients for healthy–healthy combination increased to around 0.92, and the correlation between the shape of malaria and healthy cells reduces to 0.82, making the probability of correct classifications higher (see Table 1). Our experiments indicate that use of thickness information at multiple axial planes will lead to a better probability of identification.

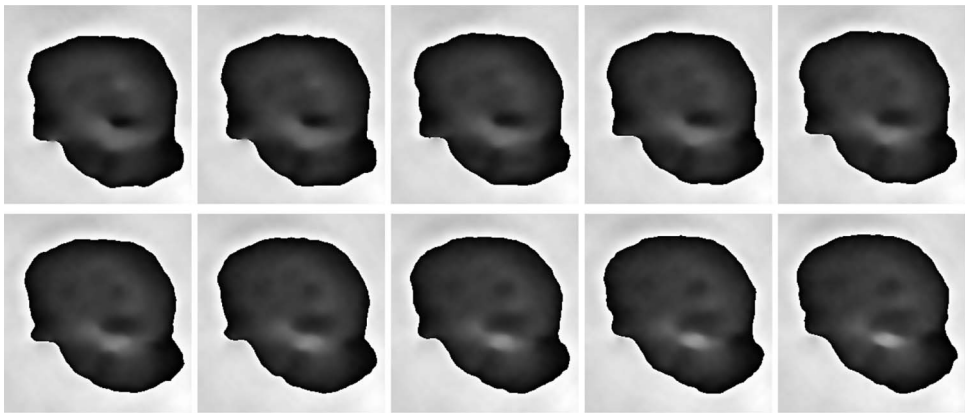

Fig. 9. Phase-contrast images of a malaria-infected RBC obtained at various axial distances. The distance between successive axial planes was 0.24 μm.

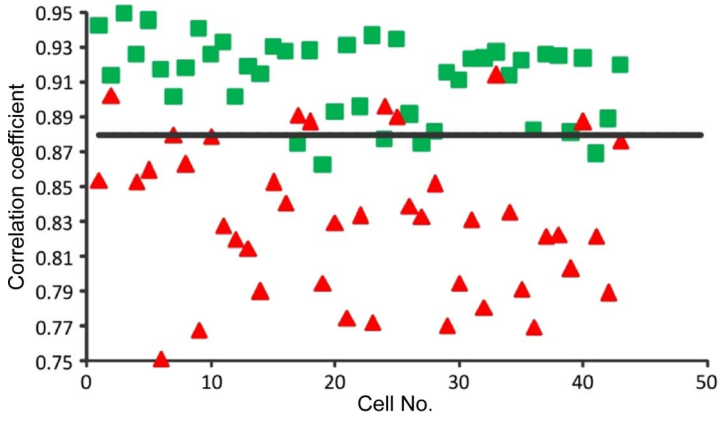

Fig. 10. Average correlation coefficient from shape comparison of different cell pairs using data from 20 axial planes (■ healthy, ▲ malaria infected, — threshold).

Fig. 11 shows the receiver operating characteristic (ROC) curves for the detection of malaria-infected RBCs using the described technique. Individual points on the ROC space represent probability for false positive (FP) identification and true positive (TP) identification.

Refractive index of blood plasma and the RBC could vary from person to person. To determine the effect of variation in refractive index on the discrimination process, simulations were carried out. For simulations, RBCs were modeled as hemispherical objects with a depression at the center. Malarial parasites were modeled as spheres having refractive index different than that of plasma and RBC. They were introduced at random positions inside the RBCs. A variation of up to 5% was also introduced to the refractive index of RBC, plasma, and the malarial parasite for each simulated cell (for both healthy and malaria-infected cells). Holograms of these objects were simulated, and then, the thickness profiles were computed with constant refractive index for plasma (1.34) and the cell (1.42). The probability of discrimination was found to be 86% using these refractive index values. With the correct refractive index values, the results improved to about 91%. It shows that the use of constant refractive index results in higher error in the discrimination probability. Simultaneous determination of refractive index and thickness may then result in improved discrimination probability [14]. But since the main aim of this work was to develop DHM as an automatic tool for identification of malaria, this aspect was not considered.

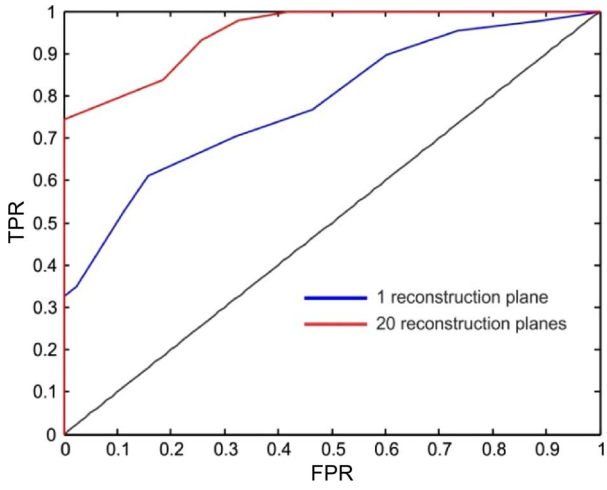

Fig. 11. ROC curves for the detection of malaria-infected RBCs using shape correlation with DHIM.

5. Conclusion and Future Scopes

Integration of DHM for sensing RBCs and correlation algorithms applied to the data has the potential to be an automated technique that can discriminate between different classes of RBCs. Comparison of the shape of the test cell with the database of healthy and infected cells may indicate whether the cell is healthy or not. Our experiments show that by using thickness profile from multiple axial planes, the recognition performance can be improved. Future of the work lies in using the technique to study other diseases affecting RBCs. Also, the use of extended focus imaging to extract information along the focus in a single shot will make the method faster [23]. A database of healthy and diseased cells can be made, and a test cell can be compared with this database to determine its state of health.

References

[1] U. Schnars and W. Jueptner, *Digital Holography: Digital Hologram Recording, Numerical Reconstruction and Related Techniques*. Berlin, Germany: Springer-Verlag, 2005.
[2] E. Cuche, F. Bevilacqua, and C. Depeursinge, "Digital holography for quantitative phase-contrast imaging," *Opt. Lett.*, vol. 24, no. 5, pp. 291–293, Mar. 1999.
[3] P. Marquet, B. Rappaz, P. J. Magistretti, E. Cuche, Y. Emery, T. Colomb, and C. Depeursinge, "Digital holographic microscopy: A noninvasive contrast imaging technique allowing quantitative visualization of living cells with subwavelength axial accuracy," *Opt. Lett.*, vol. 30, no. 5, pp. 468–470, Mar. 2005.
[4] Y. Frauel, T. Naughton, O. Matoba, E. Tahajuerce, and B. Javidi, "Three dimensional imaging and display using computational holographic imaging," *Proc. IEEE*, vol. 94, no. 3, pp. 636–653, Mar. 2006.
[5] P. Ferraro, S. Grilli, D. Alfieri, S. De Nicola, A. Finizio, G. Pierattini, B. Javidi, G. Coppola, and V. Striano, "Extended focused image in microscopy by digital holography," *Opt. Exp.*, vol. 13, no. 18, pp. 6738–6749, Sep. 2005.
[6] A. Anand, V. K. Chhaniwal, and B. Javidi, "Real-time digital holographic microscopy for phase contrast 3D imaging of dynamic phenomena," *J. Display Technol.*, vol. 6, no. 10, pp. 500–505, Oct. 2010.
[7] A. Anand, V. K. Chhaniwal, and B. Javidi, "Imaging embryonic stem cell dynamics using quantitative 3D digital holographic microscopy," *IEEE Photon. J.*, vol. 3, no. 3, pp. 546–554, Jun. 2011.
[8] B. Rappaz, A. Barbul, Y. Emery, R. Korenstein, C. Depeursinge, P. J. Magistretti, and P. Marquet, "Comparative study of human erythrocytes by digital holographic microscopy, confocal microscopy," *Cytometry Part A*, vol. 73, no. 10, pp. 895–903, Oct. 2008.
[9] D. Shin, M. Daneshpanah, A. Anand, and B. Javidi, "Optofluidic system for three dimensional sensing and identification of micro-organisms with digital holographic microscopy," *Opt. Lett.*, vol. 35, no. 23, pp. 4066–4068, Dec. 2010.
[10] G. Popescu, T. Ikeda, R. R. Dasari, and M. S. Feld, "Diffraction phase microscopy for quantifying cell structure and dynamics," *Opt. Lett.*, vol. 31, no. 6, pp. 775–777, Mar. 2006.
[11] G. Popescu, L. P. Deflores, J. C. Vaughan, K. Badizadegan, H. Iwai, R. R. Dasari, and M. S. Feld, "Fourier phase microscopy for investigation of biological structures and dynamics," *Opt. Lett.*, vol. 29, no. 21, pp. 2503–2505, Nov. 2004.
[12] Y. K. Park, M. Diez-Silva, G. Popescu, G. Lykotrafitis, W. Choi, M. S. Feld, and S. Suresh, "Refractive index maps and membrane dynamics of human red blood cells parasitized by Plasmodium falciparum," *Proc. Natl. Acad. Sci.*, vol. 105, no. 37, pp. 13 730–13 735, Sep. 2008.

[13] Y. K. Park, M. Diez, D. Fu, G. Popescu, W. Choi, I. Barman, S. Suresh, and M. S. Feld, "Static and dynamic light scattering of healthy and malaria parasite invaded red blood cells," *J. Biomed. Opt.*, vol. 15, no. 2, pp. 020506-1–020506-8, Mar./Apr. 2010.
[14] M. Mir, K. Tangella, and G. Popescu, "Blood testing at the single cell level using quantitative phase and amplitude microscopy," *Biomed. Opt. Exp.*, vol. 2, no. 12, pp. 3259–3266, Dec. 2011.
[15] M. Mir, H. Ding, Z. Wang, J. Reedy, K. Tangella, and G. Popescu, "Blood screening using diffraction phase cytometry," *J. Biomed. Opt.*, vol. 15, no. 2, p. 027016, Mar./Apr. 2010.
[16] A. Anand, V. K. Chhaniwal, and B. Javidi, "Quantitative cell imaging using single beam phase retrieval method," *J. Biomed. Opt.*, vol. 16, no. 6, p. 060503, Jun. 2011.
[17] A. Anand and B. Javidi, "Three dimensional microscopy with single beam wavefront sensing and reconstruction from volume speckle fields," *Opt. Lett.*, vol. 35, no. 5, pp. 766–768, Mar. 2010.
[18] J. W. Goodman, *Introduction to Fourier Optics*. New York: McGraw-Hill, 1996.
[19] M. Hammer, D. Schweitzer, B. Michel, E. Thamm, and A. Kolb, "Single scattering by red blood cells," *Appl. Opt.*, vol. 37, no. 31, pp. 7410–7418, Nov. 1998.
[20] P. Ferraro, S. Grilli, L. Miccio, D. Alfieri, S. De Nicola, A. Finizio, and B. Javidi, "Full color 3-D imaging by digital holography and removal of chromatic aberrations," *J. Display Technol.*, vol. 4, no. 1, pp. 97–100, Mar. 2008.
[21] S. De Nicola, A. Finizio, G. Pierattini, D. Alfieri, S. Grilli, L. Sansone, and P. Ferraro, "Recovering correct phase information in multiwavelength digital holographic microscopy by compensation for chromatic aberrations," *Opt. Lett.*, vol. 30, no. 20, pp. 2706–2708, Oct. 2005.
[22] A. Mahalanobis, "Review of correlation filters and their application for scene matching," in *Proc SPIE*, 1996, vol. CR65, pp. 240–260.
[23] M. Paturzo and P. Ferraro, "Creating an extended focus image of a tilted object in Fourier digital holography," *Opt. Exp.*, vol. 17, no. 22, pp. 20 546–20 552, Oct. 2009.